THE JOURNAL OF BIOLOGICAL CHEMISTRY
Vol. 280, No. 18, Issue of May 6, pp. 18108–18119, 2005
Printed in U.S.A.

HSP25 Inhibits Protein Kinase Cδ-mediated Cell Death through Direct Interaction*

Received for publication, January 31, 2005, and in revised form, February 23, 2005
Published, JBC Papers in Press, February 24, 2005, DOI 10.1074/jbc.M501131200

Yoon-Jin Lee‡§, Dae-Hoon Lee‡§, Chul-Koo Cho‡, Sangwoo Bae‡, Gil-Ja Jhon¶, Su-Jae Lee‖, Jae-Won Soh, and Yun-Sil Lee‡ ‡‡**

*From the ‡Laboratory of Radiation Effect and ‖Laboratory of Experimental Radiation Therapeutics, Korea Institute of Radiological and Medical Sciences, Seoul 139-706, ¶Division of Molecular Life Science, Ewha Woman's University, Seoul 120-750, and **Laboratory of Signal Transduction, Department of Chemistry, Inha University, Incheon, 402-751 Seoul, Korea*

Heat shock protein 25 (HSP25) interferes negatively with apoptosis through several pathways that involve its direct interaction with cytochrome *c* or Akt. Here we show that HSP25 inhibits protein kinase C (PKC) δ-mediated cell death through direct interaction. HSP25 binds to kinase-active PKCδ to inhibit its kinase activity and translocation to the membrane, which results in reduced cell death. Deletion constructs of HSP25 and PKCδ identified amino acids 90–103 of HSP25 and the C-terminal V5 region of PKCδ as binding sites. In addition, the interaction between HSP25 and PKCδ induced HSP25 phosphorylation at Ser-15 and Ser-86, and these phosphorylations permitted HSP25 release from PKCδ. Based on these observations, we propose that after PKCδ activation, HSP25 binds to the exposed V5 region of PKCδ. This novel function of HSP25 accounts for its cytoprotective properties via the inhibition of PKCδ and the enhancement of HSP25 phosphorylation.

Small heat shock protein (HSP)[1] has been suggested to protect cells against apoptotic cell death triggered by hyperthermia, ionizing radiation, oxidative stress, Fas ligand, and cytotoxic drugs (1–5). Several mechanisms have been proposed to account for HSP27-mediated apoptotic protection, for example, via its specific interaction with cytochrome *c* released from mitochondria into the cytosol, which prevents apoptosome formation (6, 7). The elimination of unfolded protein via the extralysosomal, energy-dependent, ubiquitin-proteasome degradation pathway is another mechanism that contributes to cell protection from stressful stimuli (8). HSP27 binds to polyubiquitin chains as well as 26 S proteasomes, and the ubiquitin-proteasome pathway is involved in the activation of transcription factor NF-κB by degrading its main inhibitor I-κBα (8).

Moreover, phosphorylated HSP27 has been shown to bind an adaptor protein Daxx and then to inhibit Fas-mediated apoptosis (9). Interaction between HSP27 and Akt is necessary for Akt activation, and this is followed by dissociation of phosphorylated HSP27 from Akt (10).

We reported recently that the radioprotective effect of HSP25 involves delayed cell growth (11, 12) and HSP25-mediated Mn-SOD gene expression (13, 14). HSP25 overexpression down-regulates ERK1/2 expression, and HSP25-mediated ERK2 suppression is involved in HSP25-induced radioresistance and cell cycle delay (15). In addition, attenuated oxidative stress-induced apoptosis by HSP25 overexpression was found to be due to the inhibition of the PKCδ-mediated ERK1/2 pathway and to the induction of the Mn-SOD gene (14), and HSP25 also inhibits radiation-induced PKCδ-mediated reactive oxygen species production (16).

Radiation and many anticancer drugs are known to kill tumor cells by inducing apoptosis. However, a defect in the apoptotic process can lead to resistance to anticancer drugs or radiotherapy. Several members of the protein kinase C (PKC) family serve as substrates for caspases, and the PKCδ isozyme has been intimately associated with apoptosis. The activation of PKCδ was found to be associated with cell cycle progression inhibition (17), and PKCδ down-regulation was found to be associated with tumor promotion (18), suggesting that PKCδ may have a negative effect on cell survival. In addition, the proteolytic activation of PKCδ has since been associated with the apoptosis induced by DNA damage, including that caused by UV light, ionizing radiation, cisplatin, etoposide, arabinoside, and doxorubicin (19–24). Moreover, several investigators have confirmed that the ectopic expression of the PKCδ catalytic fragment results in cell death (25–28). Mizuno *et al.* (26) showed that the kinase activity of a PKCδ catalytic fragment during apoptosis may be a key participant in the late stages of apoptosis.

In the present study, we observed for the first time that HSP25 binds directly to the V5 region of kinase-active PKCδ. This results in a dual form of HSP25-mediated cytoprotection, namely via the inhibition of PKCδ activity, thereby blocking apoptosis, and via the phosphorylation of HSP25, which increases its cytoprotective effect. In addition, these two types of HSP25-mediated apoptotic expression were found to be triggered by radiation or oxidative stress.

MATERIALS AND METHODS

Reagents—Rottlerin (PKCδ inhibitor), phorbol 12-myristate 13-acetate, and H_2O_2 were purchased from Calbiochem. Anti-HSP27, anti-phospho-HSP27 (Ser-15), anti-phospho-HSP27 (Ser-82), anti-HA, anti-PKCδ, anti-

* This work was supported by the Korean Institute of Science and Technology Evaluation and Planning and by the Ministry of Science and Technology through the National Nuclear Technology Program. The costs of publication of this article were defrayed in part by the payment of page charges. This article must therefore be hereby marked "*advertisement*" in accordance with 18 U.S.C. Section 1734 solely to indicate this fact.

§ Both authors contributed equally to this work.

‡‡ To whom correspondence should be addressed: Laboratory of Radiation Effect, Korea Institute of Radiological and Medical Sciences, 215-4 Gongneung-Dong, Nowon-Ku, Seoul 139-706, Korea. Tel.: 82-2-970-1325; Fax: 82-2-970-2402; E-mail: yslee@kcch.re.kr.

[1] The abbreviations used are: HSP, heat shock protein; PKC, protein kinase C; GST, glutathione *S*-transferase; HA, hemagglutinin; PMA, phorbol 12-myristate 13-acetate; SOD, superoxide dismutase; MBP, myelin basic protein; PI, propidium iodide; RFP, red fluorescent protein; GFP, green fluorescent protein; CAT, chloramphenicol acetyltransferase; FBS, fetal bovine serum; PBS, phosphate-buffered saline; MAPK, mitogen-activated protein kinase; RIF, radiation-induced fibrosarcoma; siRNA, small interfering RNA; ATPγS; adenosine 5′-*O*-(thiotriphosphate); Gy, gray; WT, wild type.

lamin B, anti-β-actin, and anti-GFP antibodies were from Santa Cruz Biotechnology (Santa Cruz, CA). Phospho-PKCδ (Ser-643) and phospho-PKCδ (pan) were from Cell Signaling Technology (Beverly, MA). Anti-phosphotyrosine antibody, PKCδ protein (recombinant protein expressed in Sf21), and PKC lipid activator were purchased from Upstate Biotechnology, Inc. (Lake Placid, NY). ATP and ATPγS were from Sigma. DsRed polyclonal antibody was from BD Biosciences.

Plasmids—Wild type mouse HSP25 (GenBank™ accession number XM124655) was cloned into pcDNA4HisMaxC (Invitrogen), which contains an N-terminal His tag. The phosphorylation mutant constructs HSP25 (S15A), HSP25 (S15D), HSP25 (S86A), HSP25 (S86D), HSP25 (S15A/S86A), and HSP25 (S15D/S86D) were constructed by PCR (29) by using the overlap extension primers. Serine was replaced by alanine or aspartate to generate the phosphorylation-deficient or phosphorylation-mimicking mutants of HSP25, respectively. The dimerization mutant HSP25 (C141A) was constructed using the same method. PCR products were digested with EcoRI and cloned into the EcoRI site of pcDNA4HisMaxC to construct expression vectors of the His-tagged mutant HSP25 protein. PCR products were also cloned into pEGFP-N1 vector (Clontech) to express GFP-tagged mutant HSP25 proteins. The internal deletion mutants were constructed in HSP25-containing pcDNA4HisMaxC vector by introducing two SalI sites in the HSP25-coding sequence using deletion primers. This was followed by restriction and ligation steps. For the HSP25-(92–145)-GFP construct, HSP25-(91–187) was amplified by PCR, and the PCR products obtained were digested and cloned into pEGFP-N1 vector (Clontech).

Wild type PKCδ (GenBank™ accession number AY545076), the regulatory domain (amino acids 2–333, REG), the catalytic domain (amino acids 334–674, CAT), and the dominant-negative catalytic domain (amino acids 334–674, CAT-KR) were cloned into pHACE that contains a C-terminal HA tag (30). To construct the PKCδ-truncated mutants, each DNA fragment was amplified using mutagenic primers containing an EcoRI site by PCR. The amplified PKCδ mutants were cloned into pHACE. The phosphorylation mutants of the catalytic domain, *i.e.* CAT (S643A), CAT (S643D), CAT (S662A), CAT (S662D), CAT (S643A/S662A), CAT (S643D/S662D), CAT-KR (S643A), CAT-KR (S643D), CAT-KR (S662A), CAT-KR (S662D), CAT-KR (S643A/S662A), and CAT-KR (S643D/S662D) were constructed using the method used for the HSP25 phosphorylation mutants. The PCR products were digested with EcoRI and cloned into the EcoRI site of pHANE, which contains an N-terminal HA tag (30). PKCδ construct was cloned into the EcoRI site of pDsRed1-N1 vector (Clontech) to express PKCδ-RFP (V5-RFP). All the primer sequences are available by request.

Cell Culture—L929 (murine fibroblasts), radiation-induced fibrosarcoma (RIF) cells, and TR (a thermoresistant clone of RIF) were cultured in Dulbecco's minimal essential medium (Invitrogen) supplemented with heat-inactivated 10% fetal bovine serum (FBS, Invitrogen) and antibiotics at 37 °C in a 5% CO_2 humidified incubator. The human non-small cell lung cancer cell lines H460, H596, and H1299 and Jurkat T leukemia cells were grown in RPMI 1640 supplemented with 10% FBS, glutamine, HEPES, and antibiotics at 37 °C in a 5% CO_2 humidified incubator. L929 and Jurkat transformant clones were obtained by stable transfection with pHSP6 (containing the complete genomic sequence of murine *HSP25*) and pBC vector (Stratagene, La Jolla, CA) (11, 12, 16) or with the MFG retroviral vector (31).

Irradiation—Cells were plated in 60-mm dishes and incubated at 37 °C in humidified 5% CO_2 in culture medium until 70–80% confluent. Cells were then exposed to γ-rays from a ^{137}Cs γ-ray source (Atomic Energy of Canada, Ltd.) at 3.81 Gy/min.

Flow Cytometric Analysis—Cells were cultured, harvested at the indicated times, stained with propidium iodide (PI), according to the manufacturer's protocol, and then analyzed using a FACScan flow cytometer (BD Biosciences).

Cytoplasmic/Nuclear Fractionation—Cells (1×10^6) grown on 10-cm tissue culture dishes were washed once with ice-cold PBS and harvested with a scraper. Cell pellets were then resuspended in hypotonic buffer (10 mM HEPES, 10 mM KCl, 0.1 mM EDTA, 0.1 mM EGTA, 0.5% Nonidet P-40) and incubated at 4 °C for 15 min. Samples were agitated every 5 min and then centrifuged at 12,000 rpm for 30 s to collect the cytoplasmic fraction. Pellets were resuspended, incubated in nuclear extraction buffer (20 mM HEPES, 20% glycerol, 0.42 M NaCl, 1 mM EDTA, 1 mM EGTA) for 30 min, and centrifuged at 12,000 rpm for 20 min to obtain the nuclear fraction.

Cytosolic/Membrane Protein Fractionation—Cells were washed twice with PBS and then sonicated in buffer containing 100 mM Tris-HCl (pH 7.5), 50 mM $MgCl_2$, 10 mM dithiothreitol, and 10 mM phenylmethylsulfonyl fluoride. The sonicated cells were then incubated in ice for 1 h and ultracentrifuged for 1 h at 100,000 × *g* to separate the membrane and cytosolic fractions. The cell pellet obtained was sonicated in buffer containing 1% Triton X-100, incubated in ice for 1 h, and then ultracentrifuged for 1 h at 100,000 × *g* to separate the membrane fraction from cellular debris.

Immunofluorescence Analysis—For immunofluorescence analysis, cells were fixed with 2% paraformaldehyde, permeabilized with 0.1% Triton X-100 in PBS, and then washed three times with PBS. They were then incubated with goat anti-phospho-HSP27 (Ser-15 and Ser-82) diluted 1:200 in PBS containing 5% FBS for 1 h at room temperature in a humidified chamber. Excess antibody was removed by washing coverslips three times with PBS. Cells were then incubated with fluorescein isothiocyanate-conjugated goat anti-rabbit immunoglobulin G (IgG) (Dako, Produktionsvej, Denmark), at 1:200 dilution in PBS containing 5% FBS for 4 h, and then incubated with 0.5 μg/μl propidium iodide (Molecular Probes, Inc., Eugene, OR) for 5 min at room temperature. After washing three times with PBS, coverslips were mounted onto microscope slides using ProLong antifade mounting reagent (Molecular Probes), and slides were analyzed under a confocal laser-scanning microscope (Leica Microsystems).

PAGE and Western Blotting—For PAGE and Western blotting, cells were solubilized with lysis buffer (120 mM NaCl, 40 mM Tris (pH 8.0), 0.1% Nonidet P-40) and boiled for 5 min, and equal amounts of protein were analyzed on 10% SDS-PAGE. After electrophoresis, proteins were to a nitrocellulose membrane and processed for immunoblotting. Blots were further incubated with horseradish peroxidase-conjugated secondary antibody diluted at 1:5,000, and specific bands were visualized by chemiluminescence (ECL, Amersham Biosciences). Autoradiographs were recorded on X-Omat AR film (Eastman Kodak Co.).

PKC Kinase Assay—Cellular proteins were extracted using PKC extraction buffer (50 mM HEPES (pH 7.5), 150 mM NaCl, 0.1% Tween 20, 1 mM EDTA, 2.5 mM EGTA, and 10% glycerol) containing protease inhibitors (10 μg/ml each of aprotinin and leupeptin and 0.1 mM phenylmethylsulfonyl fluoride) and phosphatase inhibitors (1 mM NaF, 0.1 mM Na_3VO_4, and 10 mM β-glycerophosphate). HA-tagged PKC proteins from 300 μg of cell extracts were immunoprecipitated with 3 μg of anti-HA antibody and 30 μl of protein G-Sepharose for 3 h at 4 °C. The immunoprecipitates were washed twice with PKC extraction buffer and PKC reaction buffer (50 mM HEPES (pH 7.5), 10 mM $MgCl_2$, 1 mM dithiothreitol, 2.5 mM EGTA, 1 mM NaF, 0.1 mM Na_3VO_4, and 10 mM β-glycerophosphate) and then resuspended in 20 μl of PKC reaction buffer. The kinase assay was initiated by adding 40 μl of PKC reaction buffer containing 5 μg of dephosphorylated MBP protein (Upstate Biotechnology, Inc.) or His-HSP25 protein and 5 μCi of [γ-^{32}P]ATP. Reactions were carried out for 30 min at 30 °C and terminated by adding SDS sample buffer. Mixtures were then boiled for 5 min, and the reaction products were analyzed by SDS-PAGE and autoradiography.

Preparation of Recombinant HSP25 Proteins—Vectors for the expression of recombinant HSP25 were prepared by inserting the *HSP25* wild type into the NcoI-EcoRI restriction site of pProExHTa vector (Invitrogen). The resulting plasmid was transformed into *Escherichia coli* BL21 (Novagen) to produce His tag-HSP25 fusion proteins (His-HSP25) after treating with 0.15 M isopropyl-1-thio-β-D-galactopyranoside for 4 h at 30 °C. Bacteria were lysed in a buffer containing 50 mM HEPES (pH 7.5), 0.45 M NaCl, 5 mM dithiothreitol, Complete protease inhibitor (Roche Diagnostics), 1.25 mg/ml lysozyme, and 11.2 μg/ml DNase I (Sigma). His-HSP25 proteins were extracted from inclusion bodies by incubating for 1 h followed by vigorous shaking at 37 °C in 25 mM phosphate buffer, pH 7.4, containing 150 mM NaCl, 1 mM EDTA, 2% (v/v) Triton X-100, 5 mM dithiothreitol, and Complete protease inhibitor. The solubilized His-HSP27 proteins were affinity-purified using nickel-nitrilotriacetic acid-agarose beads (Qiagen).

Immunoprecipitation—Cells (1×10^7) were lysed in immunoprecipitation buffer (50 mM HEPES (pH 7.6), 150 mM NaCl, 5 mM EDTA, 0.1% Nonidet P-40). After centrifuging (10 min at 15,000 × *g*) to remove particulate material, the supernatant was incubated with antibodies (1:100) against anti-HSP27 or PKCδ with constant agitation at 4 °C. Immunocomplexes were precipitated with protein A-Sepharose (Sigma) and analyzed by SDS-PAGE by enhanced chemiluminescence (Amersham Biosciences).

Cell Transfection—Pre-designed siRNA for human HSP27 (HSPB1–3, Ambion catalog number16706) was purchased from Ambion, Inc. (Austin, TX). Cells were transfected with the siRNAs for 48 h using Lipofectamine TM 2000 (Invitrogen). A mixture of 250 μl of Opti-MEM medium (Invitrogen) and 20 μl of Lipofectamine™ 2000 was incubated for 5 min at room temperature and then combined with 100 nM of siRNA diluted with 250 μl of Opti-MEM. The resulting mixture (500 μl) was incubated for 20 min at room temperature to allow complex formation and then overlaid onto each well containing the cells to a final

volume of 2.5 ml/60-mm dish. The transient transfection of all cell types was carried out using Plus Lipofectamine™ reagent (Invitrogen) and Lipofectamine™ reagent.

Histidine Pull-down Assay in Vitro—The *in vitro* transcription and translation of PKCδ was performed using a TnT T7 Quick Master Mix kit (Promega, Madison, WI) in the presence of [^{35}S]methionine, according to the manufacturer's protocol. An aliquot of His-tagged HSP25 protein, bound to nickel-nitrilotriacetic acid-agarose beads, was incubated with 5 μl of *in vitro* translated PKCδ in 500 μl of NETN buffer (100 mM NaCl, 1 mM EDTA (pH 8.0), 20 mM Tris-HCl (pH 8.0), 0.2% Nonidet P-40, 10 mM imidazole) for 2 h. Beads were washed five times with 1 ml of NETN buffer, resuspended in Laemmli sample buffer, and subjected to SDS-PAGE before autoradiography.

Histidine Pull-down Assay—Histidine-tagged DNA constructs were transfected into the cells by using Lipofectamine Plus reagent. After incubation for 48 h, cells were harvested, and whole cell extracts were prepared as described previously. Cell extracts were mixed and incubated with nickel-nitrilotriacetic acid-agarose beads for 30 min at 4 °C in the presence of 10 mM imidazole. After washing the resin with buffer containing 10 mM imidazole, proteins were recovered by suspension in Laemmli sample buffer and then subjected to SDS-PAGE and Western blot analysis using anti-PKCδ or anti-HA antibodies.

RESULTS

Interaction between HSP25 and the Catalytic Domain of PKCδ and PKCδ Kinase Activity Is Necessary for Its Interaction with HSP25—As HSP25 overexpression was found to inhibit PKCδ activity in our previous study (14), and another HSP, HSP70, was reported to bind PKCβ (32), we examined possible binding between HSP25 and PKCδ. HSP25 was found to coimmunoprecipitate with PKCδ in whole cell lysates of L929 and Jurkat T cells overexpressing HSP25 (Fig. 1*A*). To confirm binding between PKCδ and HSP25, several deletion constructs of PKCδ were made (Fig. 1*B*). Immunoprecipitation revealed that the catalytic domain of PKCδ (CAT), but not the regulatory domain of PKCδ (REG), is an HSP25 binding target. When rottlerin, a specific PKCδ inhibitor, was pretreated, HSP25 binding disappeared, suggesting that the kinase activity of PKCδ is important for the interaction between HSP25 and PKCδ (Fig. 1*C*). A loss of binding activity after HSP25 antisense transfection confirmed the specific interaction between HSP25 and PKCδ (Fig. 1*C*), which was further confirmed by probing histidine pull downs of HSP25 using several domain mutants of PKCδ fused with a HA tag. Consistently, wild type (WT) PKCδ interacted with HSP25, and PKCδ-CAT mediated this binding (Fig. 1*D*). TR cells, which were derived as a thermoresistant clone of RIF and which show high expression levels of HSP25, were used to confirm the binding potential of endogenous HSP25 with PKCδ. Moreover, transfection of PKCδ-CAT into TR cells was found to increase the interaction between HSP25 and PKCδ-CAT (Fig. 1*E*). However, we did not detect any interaction between HSP70 and PKCδ (data not shown). Because rottlerin pretreatment completely inhibited the interaction between HSP25 and PKCδ, we hypothesized that kinase-active PKCδ is required for this interaction. Thus we transfected PKCδ-CAT-K376R (CAT-KR), which lacks PKCδ kinase activity, and performed immunoprecipitation experiments. Neither PKCδ-REG (Fig. 1*F*, *5th lane*) nor CAT-KR interacted with HSP25 (Fig. 1*F*, *4th lane*). In contrast, PKCδ-CAT bound to HSP25 (Fig. 1*F*, *3rd lane*). Moreover, pretreatment with PKC activators such as PMA or H_2O_2 increased the interaction between HSP25 and PKCδ, and this was accompanied by an increase in the MBP kinase activity of PKCδ; however, rottlerin pretreatment reduced HSP25-PKCδ binding, even though MBP phosphorylation by PKCδ was not completely inhibited (Fig. 1*G*) (H_2O_2 treatment data not shown). Because PKCδ-CAT-KR did not interact with HSP25, we used ATP and ATPγS to confirm the importance of the kinase activity of PKCδ. An interaction was observed between HSP25 and PKCδ after treating with H_2O_2, and this binding was dramatically increased by cotreating H_2O_2 with ATP. However, cotreatment with ATPγS (often regarded as a nonhydrolyzable ATP analogue and is used as an inhibitor of phosphatases and ATPases (33)) blocked this interaction (Fig. 1*H*), suggesting that PKCδ kinase activity (in terms of the binding and hydrolysis of ATP) is important for the interaction between HSP25 and PKCδ.

Interaction between PKCδ-CAT and HSP25 Inhibits PKCδ-mediated Cell Death—Because PKCδ has been reported to induce apoptosis (34), we examined if the interaction between HSP25 and PKCδ affects PKCδ-mediated apoptosis. In L929 cells cotransfected with PKCδ and HSP25, PKCδ activation by H_2O_2 was lower than in cells transfected with only PKCδ (Fig. 2*A*). In addition, the tyrosine phosphorylation of PKCδ, which correlates with its kinase activity (35) and which induces many PKCδ-mediated effects like the induction of apoptosis (36), was also inhibited by HSP25 overexpression (Fig. 2*B*). In addition, we observed that H_2O_2 treatment increased PKCδ kinase activity and that the addition of HSP25 protein to the cell lysates reduced PKCδ kinase activity (Fig. 2*C*), which shows the inhibition of PKCδ kinase activity by HSP25. PKCδ-WT increased cell death due to H_2O_2 treatment, and PKCδ-CAT appeared to mediate this effect, although PKCδ-REG and PKCδ-CAT-KR, which do not have PKCδ kinase activity, reduced H_2O_2-mediated cell death (Fig. 2*D*). Moreover, radiation-induced DNA fragmentation (Fig. 2*E*) and cytochrome *c* release to the cytosol were inhibited when cells were pretreated with rottlerin. The effect of HSP25 overexpression was similar to that of rottlerin in terms of cytochrome *c* release (Fig. 2*F*).

Amino Acids 90–103 of HSP25 and V5 Region Located in the Catalytic Domain of PKCδ Are the Binding Sites of Each Molecule—To provide definitive evidence that HSP25 prevents cell death by binding to PKCδ, several mutants of HSP25 were prepared. L929 cells were transiently transfected with an empty plasmid (control) or a plasmid containing wild type or a mutated HSP25 cDNA (refer to Fig. 3*A* for details of the mutants used). Coimmunoprecipitation studies demonstrated that deletion mutants HSP25-(Δ90–103) and HSP25-(Δ92–145) did not bind to PKCδ-CAT, whereas HSP25 mutants Δ53–91, Δ106–132, and Δ133–142 were able to bind to PKCδ-CAT as efficiently as wild type HSP25 (Fig. 3*B*). His pull-down analysis also confirmed that amino acids 90–103 of HSP25 are necessary for PKCδ-CAT binding (data not shown). When H_2O_2-induced cell death was examined, a protective effect was observed after transfecting HSP25 Δ53–91, Δ106–132, or Δ133–142 mutants, which interacted with PKCδ-CAT like the wild type (Fig. 3*C*). However, cell death remained at the control level after transfection with HSP25-(Δ90–103) or HSP25-(Δ92–145) mutant. To identify the PKCδ binding locus, deletion constructs of PKCδ-CAT were made (refer to Fig. 3*D*) and transfected into HSP25-overexpressing L929 cells. Coimmunoprecipitation analysis revealed that the deletion mutants Δ343–629, Δ344–500, and Δ403–629 did not bind to HSP25, whereas mutant Δ373–647 bound to HSP25 as efficiently as PKCδ-CAT (Fig. 3*E*), suggesting that the amino acid sequence 630–674 (the V5 region) of PKCδ is a binding site. To determine whether the V5 region of PKCδ binds directly to the amino acid sequence 90–103 of HSP25, immunoprecipitation was performed using a GFP-tagged 90–103-amino acid sequence of HSP25 or an RFP-fused PKCδ V5 region. HSP25 was found to bind to PKCδ-CAT and to the V5 region, and the amino acid 90–103 sequence of HSP25 also directly bound to the PKCδ-V5 region (Fig. 3*F*). Confocal analysis also revealed the colocalization of the V5 region of PKCδ and of the amino acid 90–103 sequence of HSP25 in cytosol (data not shown). These findings demonstrate that

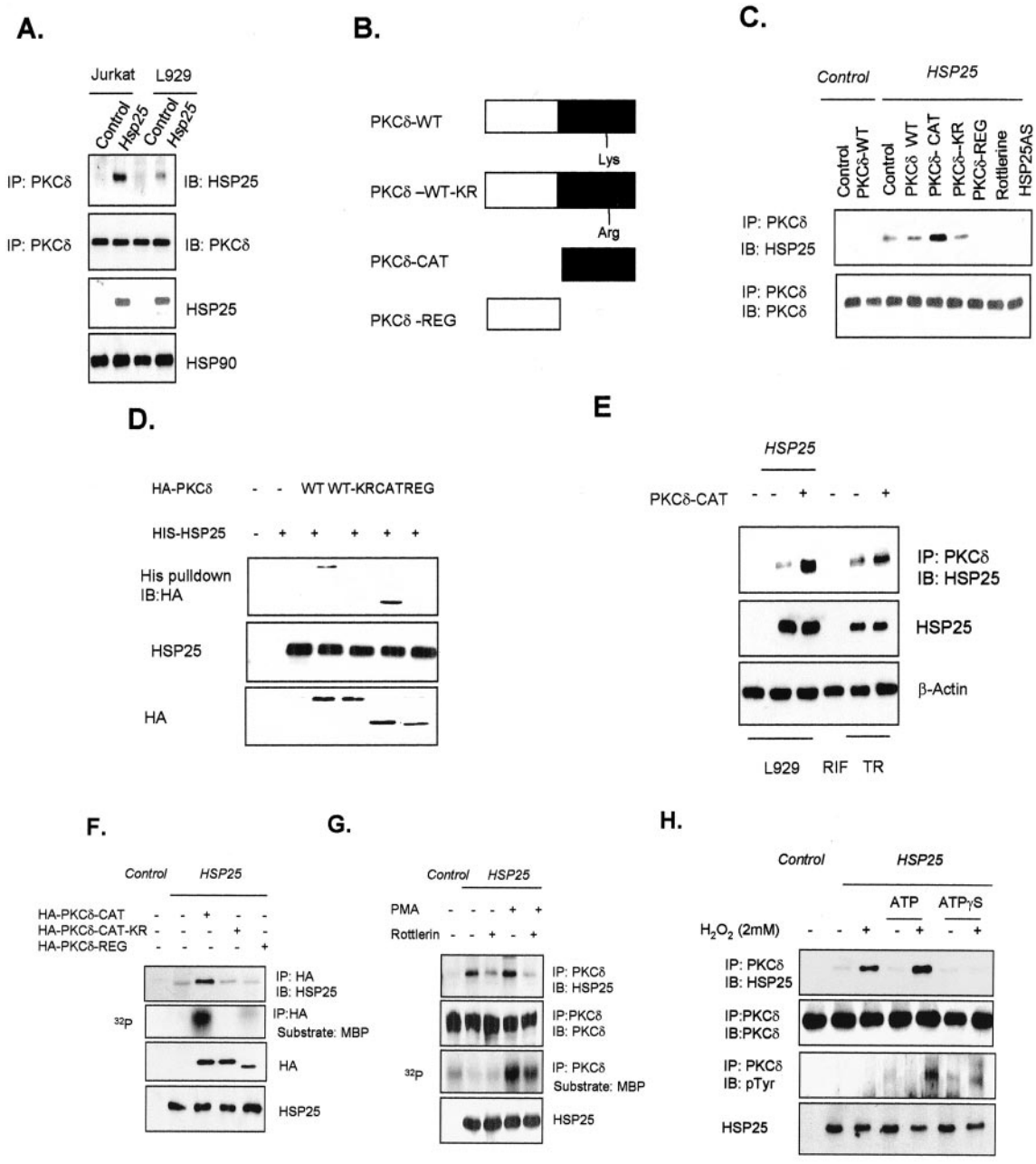

FIG. 1. **Interaction between HSP25 and kinase-active PKCδ catalytic domain.** *A*, immunodetection of HSP25 or PKCδ in control and in HSP25-overexpressing L929 cells or Jurkat T cells, with previous immunoprecipitation (*IP*) of PKCδ. *B*, schematic drawing of PKCδ point or deletion mutants. Wild type PKCδ (*PKCδ-WT*), Lys-Arg point mutant of wild type PKCδ (*PKCδ-WT-KR*), regulatory domain deleted mutant of PKCδ (*PKCδ-CAT*), catalytic domain deleted mutant (*PKCδ-REG*). *C*, after immunoprecipitation of PKCδ in lysates from control or HSP25-overexpressed L929 cells transfected with the indicated HA-tagged PKCδ point or deletion mutants or the HSP25 antisense construct (*HSP25AS)*, or pretreated with rottlerin (5 μM), the immunodetection of HSP25 and PKCδ was performed. *D*, the indicated HA-tagged PKCδ deletion mutants were transfected to L929 cells, and cell lysates were incubated with immobilized His-HSP25 or His vector. Retained HA proteins were detected by Western blotting using an anti-HA antibody. His fusion proteins are also shown. The transfection efficiencies of HA-tagged or HSP25 vectors were confirmed by Western blotting using anti-HA or anti-HSP25 antibody. *E*, PKCδ was immunoprecipitated in lysates from control or HSP25-overexpressing L929 cells, RIF, or TR (thermoresistant clone of RIF) cells with or without PKCδ-CAT transfection, and HSP25 was immunodetected. *F*, immunoprecipitation of HA in lysates from control or HSP25-overexpressing L929 cells after transfecting HA-tagged PKCδ-CAT, PKCδ-CAT-KR, or PKCδ-REG vectors. HSP25 protein was immunodetected using anti-HSP25 antibody. Cellular proteins were extracted after lysing with PKC extraction buffer. HA-tagged PKC proteins from 300 μg of cell extracts were immunoprecipitated using an anti-HA antibody and protein G-Sepharose. Immune complex kinase reactions were performed in the presence of GST-MBP substrate and [γ-^{32}P]ATP. The transfection efficiencies of HA-tagged or HSP25 vectors were confirmed by Western blotting using anti-HA or anti-HSP25 antibody. *G*, immunoprecipitation of PKCδ in lysates from control or HSP25-overexpressing L929 cells 30 min after adding PMA (100 nM) with or without pretreatment with rottlerin (5 μM) for 30 min, followed by HSP25 or PKCδ immunodetection using anti-HSP25 or anti-PKCδ antibodies. Cellular proteins were extracted after lysing with PKC extraction buffer. HA-tagged PKC proteins from 300 μg cell extracts were immunoprecipitated using an anti-HA antibody and protein G-Sepharose. Immune complex kinase reactions were performed in the presence of GST-MBP substrate and [γ-^{32}P]ATP. *H*, immunoprecipitation of PKCδ in lysates of control or HSP25-overexpressing L929 cells pretreated with H_2O_2 (2 mM) with or without ATP or ATPγS (100 μM) pretreatment. Protein extracts (500 μg) were immunoprecipitated with anti-PKCδ antibody, and immunodetection was performed using anti-phosphotyrosine (*p-Tyr*) antibody. *IB*, immunoblot.

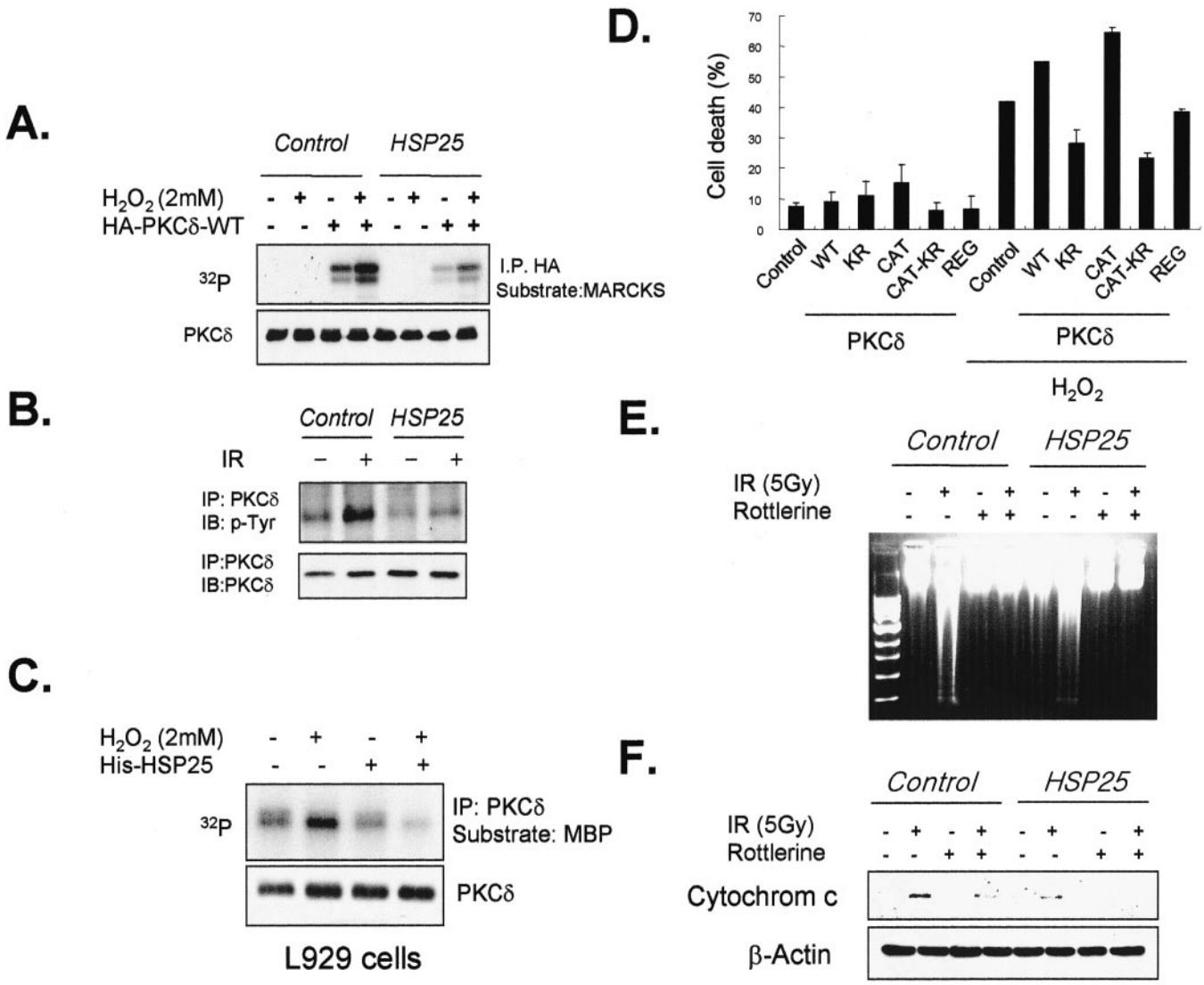

FIG. 2. **Interaction of PKCδ-CAT with HSP25 inhibits PKCδ-mediated apoptosis.** *A*, control and HSP25-overexpressing L929 cells were transfected with PKCδ-WT and treated with or without H_2O_2 (2 mM). Cells were then lysed, and cellular proteins were extracted. HA-tagged PKCδ proteins were immunoprecipitated (*IP*) from 300 μg of cell extracts by using an anti-HA antibody and protein G-Sepharose. Immune complex kinase reactions were performed in the presence of GST-myristoylated alanine-rich C kinase substrate (*MARCKS*) and [γ-^{32}P]ATP. *B*, protein extracts (500 μg) from control and HSP25-overexpressing L929 cells were immunoprecipitated with anti-PKCδ antibody and immunodetected using anti-phosphotyrosine (*p-Tyr*) antibody. *C*, cellular proteins from L929 cells pretreated with H_2O_2 (2 mM) with or without His-tagged HSP25 protein (15 μg) were extracted by lysis with PKC extraction buffer. HA-tagged PKCδ proteins were immunoprecipitated from 300 μg of cell extracts using an anti-PKCδ antibody and protein G-Sepharose. Immune complex kinase reactions were performed in the presence of GST-MBP substrate and [γ-^{32}P]ATP. *D*, the cell deaths of L929 cells transfected with the indicated PKCδ deletion mutants with or without treatment of H_2O_2 (2 mM) for 4 h were followed by flow cytometry after PI staining. Results are the means ± S.D. of two independent experiments. DNA samples from control and HSP25-overexpressing L929 cells treated with 5-Gy gamma rays for 72 h and with or without rottlerin (5 μM) pretreatment were extracted from cells, subjected to agarose gel electrophoresis, stained with ethidium bromide, and visualized under UV light (*E*). Protein extracts were isolated, and Western blotting was performed using anti-cytochrome *c* antibody (*F*). *IB*, immunoblot.

amino acids 90–103 of HSP25 are a binding site for the V5 region of PKCδ.

HSP25 Binds to the Unphosphorylated PKCδ-V5 Region and Inhibits PKCδ Membrane Translocation—Binding between HSP70 and PKCβ II is dependent on the phosphorylation status of PKCβ II (32), and several autophosphorylation sites have been identified in the V5 region of PKCδ (37–40). Moreover, PKC activation has been reported to regulate the autophosphorylation of these sites (37, 38). To elucidate whether autophosphorylation status affects the interaction between HSP25 and PKCδ, we generated Ser-643 and Ser-662 phosphorylation-deficient and phosphorylation-mimicking mutants of PKCδ-CAT. Coimmunoprecipitation revealed that the phosphorylation-deficient mutants (S643A, S662A, and S643A/S662A) bound to HSP25, whereas the phosphorylation-mimicking mutants (S643D, S662D, and S643D/S662D) did not, suggesting that the nonphosphorylated form of PKCδ V5 is important for HSP25 binding (Fig. 4*A*). In the case of PKCδ-CAT-KR, which does not have kinase activity, all mutants failed to bind HSP25 (Fig. 4*A*). His pull-down analysis was used to confirm the above results. Because it has been reported that the autophosphorylation of the V5 region affects the membrane translocation of PKC (41), we examined PKCδ phosphorylation status at Ser-643 and Ser-662. After treating the cells with H_2O_2 for 30 min, phosphorylated PKCδ at Ser-643 and Ser-662 was translocated to the particulate fraction, and this was sustained 60 min later. However, in the case of HSP25-overexpressing cells, no phosphorylated PKCδ was translocated to the particulate fraction in accompaniment with the reduced total amount of phosphorylated PKCδ (Fig. 4*B*), which suggests that the interaction

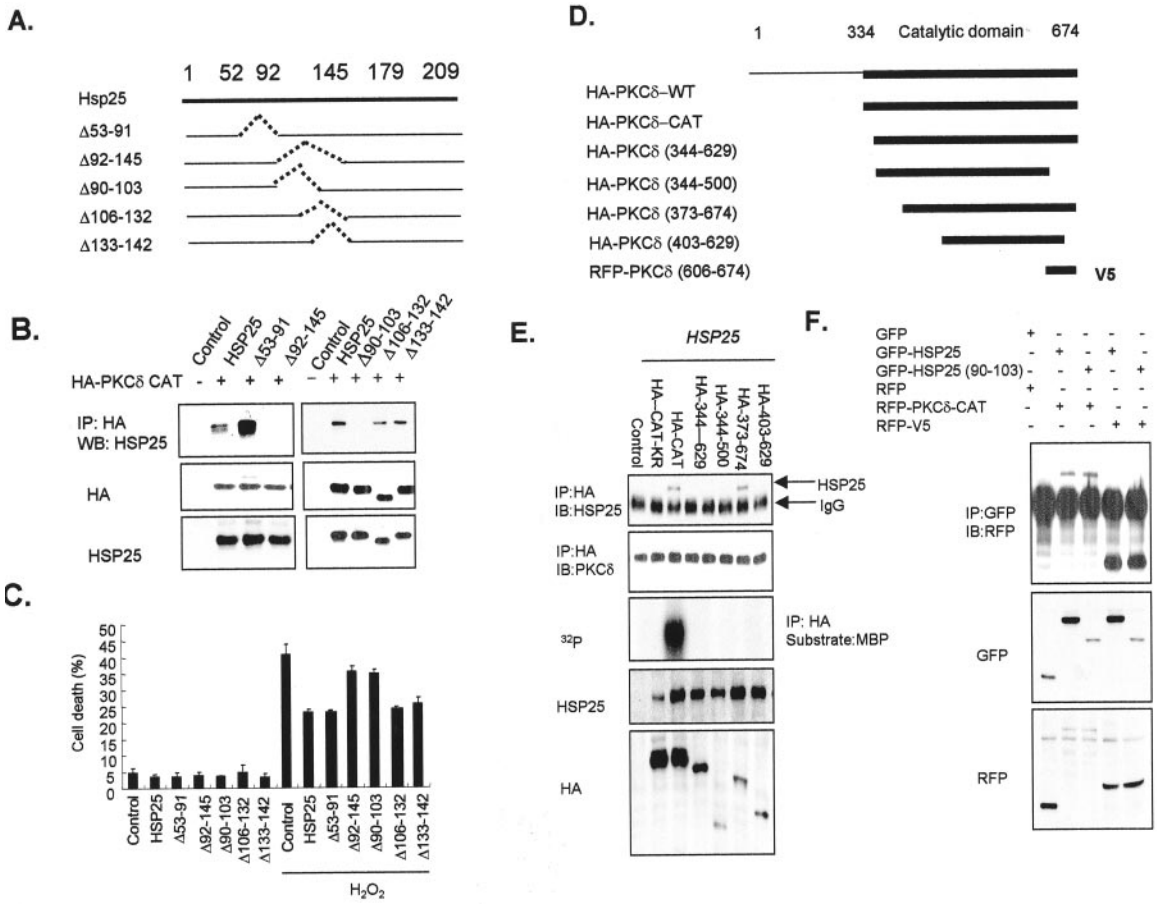

FIG. 3. **Characterization of binding sites of HSP25 and PKCδ.** *A*, schematic drawing of the HSP27 deletion mutants used in this study. Deleted amino acids are indicated by *dotted lines*. *B*, immunodetection of HSP25 in lysates after immunoprecipitation (*IP*) of HA in L929 cells cotransfected with HA-tagged PKCδ-CAT and with control vector, or vectors containing either wild type HSP25 cDNA or the mutants described in *A*, was performed. The transfection efficiencies of HA-tagged or HSP25 mutant vectors were confirmed by Western blotting (*WB*) using anti-HA or anti-HSP25 antibody. *C*, the cell deaths of L929 cells transfected with wild type or mutant HSP25 vectors, as described in *A*, with or without H_2O_2 (2 mM) treatment for 4 h were measured by flow cytometry after PI staining. Results are the means ± S.D. of three independent experiments. *D*, schematic drawing of the PKCδ-CAT deletion mutants used in this study. *E*, immunoprecipitation of HA and the immunodetection of HSP25 and PKCδ in control or HSP25-overexpressing L929 cell lysates after transfection with various HA-tagged PKCδ-CAT deletion mutants. Cellular proteins were lysed and extracted using PKC extraction buffer. HA-tagged PKC proteins from 300 μg of cell extracts were immunoprecipitated using anti-PKCδ antibody and protein G-Sepharose. Immune complex kinase reactions were performed in the presence of GST-MBP substrate and [γ-^{32}P]ATP. Transfection efficiencies were confirmed by Western blotting using anti-HA or anti-HSP25 antibody. *F*, after immunoprecipitation of GFP in the lysates of cells transfected with GFP control and GFP-fused HSP25 vectors encoding wild type or truncated amino acid 92–145 of HSP25 with or without the cotransfection of RFP-tagged control and PKCδ vectors encoding CAT or V5 region, immunodetection with anti-RFP was performed. The transfection efficiencies of GFP- or RFP-tagged vectors were confirmed by Western blotting using anti-GFP or anti-RFP antibody. *IB*, immunoblot.

between the V5 region of PKCδ and HSP25, which blocks the phosphorylation of PKCδ at Ser-643 and Ser-662, inhibits PKCδ translocation to the particulate fraction.

Binding of Kinase-active PKCδ with HSP25 Induces HSP25 Phosphorylation—PKC is a family of the phospholipid-dependent serine/threonine protein kinases, members of which activate various proteins by phosphorylation. Moreover, HSP25 is known to be phosphorylated at Ser-15 and Ser-86 by certain kinases, *e.g.* by MAPK-activated protein kinase 2/3 and by p38 MAPK (42, 43). Therefore, to elucidate whether PKCδ affects HSP25 phosphorylation status after interaction, we examined the kinetics of binding between PKCδ and HSP25, PKCδ activity, and HSP25 phosphorylation. After adding H_2O_2 to HSP25-overexpressing cells, binding of HSP25 and PKCδ was observed within 10 min and peaked at 30 min, which was similar to the PKCδ kinase activity profile (using MBP as a substrate). To determine whether PKCδ can affect HSP25 phosphorylation, PKCδ kinase activity was examined using HSP25 as a substrate in the absence or presence of [γ-^{32}P]ATP. ^{32}P incorporation was found to increase in a time-dependent manner with maximal kinase activation 90 min after adding H_2O_2, suggesting that PKCδ acts as a specific kinase for HSP25 and that it activates HSP25 after interacting with HSP25. Western blot studies on the phosphorylation status of Ser-86 and Ser-15 of HSP25, using specific antibodies, showed that HSP25 phosphorylation peaked 90 min after adding H_2O_2 (Fig. 5*A*). When PKCδ and HSP25 proteins were directly mixed in the presence of [γ-^{32}P]ATP, increased HSP25 (25 kDa) phosphorylation was accompanied by an increase in ^{32}P-labeled PKCδ (78 kDa) protein, as shown Fig. 5*B*. Increased phosphorylation of Ser-86 and Ser-15 by PMA treatment was also inhibited by rottlerin pretreatment (Fig. 5*C*). Cotransfection of HSP25 with PKCδ-CAT-KR also reduced phosphorylation at these two sites, whereas PKCδ-CAT increased the phosphorylation of HSP25 (Fig. 5*D*), which indicates that the interaction between HSP25 and PKCδ induces HSP25 phosphorylation at Ser-15 and Ser-86. Because the degree of inhibition by CAT-KR was higher at the Ser-86 site, we hypothesized that the phosphorylation of HSP25 at Ser-86 is affected more by the binding of HSP25 and PKCδ. To elucidate if the direct interaction between PKCδ and HSP25 affects HSP25 phosphorylation, S643A/S662A (serine phosphorylation sites replaced with Ala; HSP25 binding capac-

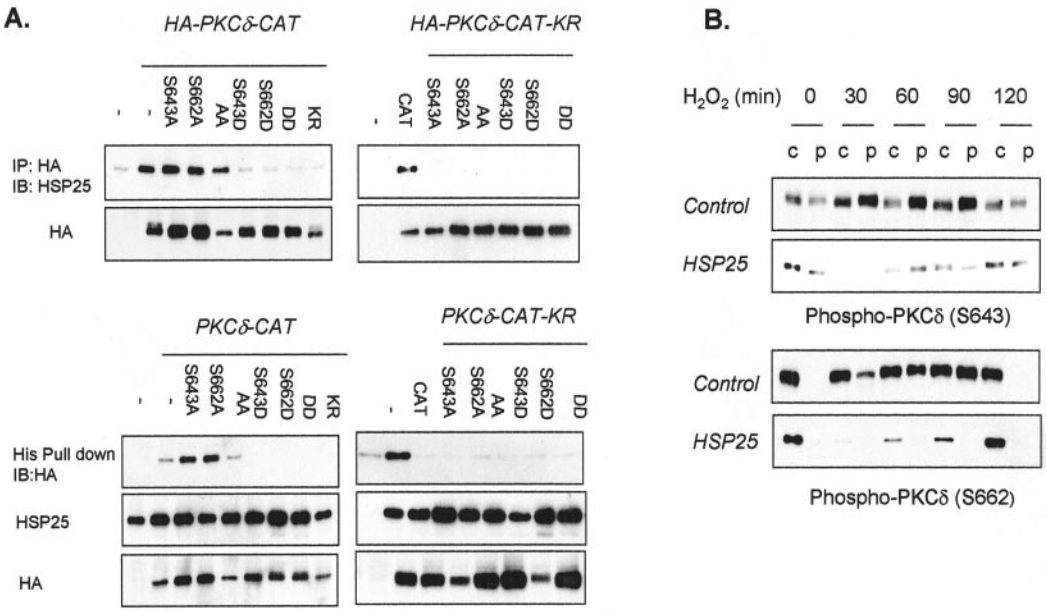

FIG. 4. **Dephosphorylation-dependent binding of the PKCδ by HSP25.** *A*, immunodetection of HSP25 (in lysates after PKCδ immunoprecipitation) of transfected L929 cells of HA-fused PKCδ-CAT or PKCδ-CAT-KR vectors containing the wild type and the indicated Ser-643 and Ser-662 point mutants. The transfection efficiencies of HA-tagged vectors were confirmed by Western blotting using anti-HA antibody (*upper panel*). Transfected L929 cells were incubated with immobilized His-HSP25 vectors. Retained HA protein was detected by Western blotting using an anti-HA antibody. His fusion proteins are also shown in the same gel. The transfection efficiencies of HA-tagged vectors were confirmed by Western blotting using anti-HA antibody. *B*, soluble and particulate fractions were isolated from control and HSP25-overexpressing L929 cells, and Western blotting was performed for PKCδ phosphorylation at Ser-643 or Ser-662 using specific antibodies. *IP*, immunoprecipitation; *IB*, immunoblot.

ity in Fig. 4*A*) or S643D/S662D (serine phosphorylation sites replaced with negatively charged Asp; no HSP25 binding capacity in Fig. 4*A*) was transfected and HSP25 phosphorylation examined. PKCδ-CAT showed both MBP kinase activity and HSP25 phosphorylation activity. PKCδ (AA) mutant showed neither MBP kinase activity nor HSP25 phosphorylation activity, but PKCδ (DD) mutant showed MBP kinase activity without HSP25 phosphorylation activity (Fig. 5*E*), suggesting that direct interaction between HSP25 and PKCδ is necessary for HSP25 phosphorylation by PKCδ.

Phosphorylated HSP25 Translates into the Nucleus and Unphosphorylated HSP25 at Ser-15 and Ser-86 Preferentially Binds to PKCδ—To determine the fate of phosphorylated HSP25 after its interaction with PKCδ, and because phosphorylated HSP25 has been reported to be translocated to the nucleus (44), we fractionated cell extracts and immunoprecipitated them with anti-PKCδ. HSP25 and PKCδ interacted in the cytosol (Fig. 6*A*), and after treating H_2O_2 this interaction increased, peaking at 30 min in the cytosol, but no interaction was observed in the nucleus. However, the nuclear translocation of phospho-HSP25 (both Ser-15 and Ser-86) was induced by H_2O_2 treatment, and a translocation peak was observed after 90 min of H_2O_2 treatment, when the interaction between HSP25 and PKCδ began to disappear (Fig. 6*B*). Confocal image analysis revealed the translocation of phospho-HSP25 to the nucleus after 90 min of H_2O_2 treatment, and this effect was stronger for the Ser-86-phosphorylated form of HSP25 (Fig. 6*C*). Because interaction between HSP25 and PKCδ occurred in the cytosol and phospho-HSP25 translocated to the nucleus, we generated phosphorylation-deficient and phosphorylation-mimicking mutants of HSP25 at Ser-15 and Ser-86 to further investigate whether PKCδ binds to unphosphorylated or phosphorylated HSP25. When HA-PKCδ-CAT was coexpressed with the His-HSP25 phospho-mutants in L929 cells, phosphorylation-deficient mutants of HSP25 (S15A and S86A) bound to PKCδ-CAT, whereas phosphorylation-mimicking mutants (S15D and S86D) did not (Fig. 6*D*). Moreover, binding of the S15A/S86A mutant of HSP25 was greater than those of the S15A or S86A mutants, implying that both sites contribute to binding. Cysteine 141 in the α-crystalline domain of HSP25, which was reported to affect HSP27 binding to cytochrome *c* (7), was not found necessary for PKCδ binding. His pull-down experiments also showed similar results, indicating that only unphosphorylated HSP25 can bind to PKCδ-CAT (data not shown). Moreover, the binding of the phosphorylation-deficient mutant S15A/S86A to PKCδ inhibited H_2O_2-induced PKCδ activation, whereas the phosphorylation-mimicking mutant (S15D/S86D), which did not bind PKCδ, did not affect H_2O_2-induced PKCδ activation (Fig. 6*E*), suggesting that unphosphorylated HSP25 binds kinase-active PKCδ and that this interaction inhibits PKCδ activity. Moreover, the interaction between unphosphorylated HSP25 and PKCδ-CAT inhibited the cell death triggered by H_2O_2 (Fig. 6*F*), suggesting that the interaction between unphosphorylated HSP25 (S15A/S86A) and PKCδ-CAT has a cytoprotective effect. HSP25 (S15D/S86D) also exhibited a cytoprotective effect even though it did not bind to PKCδ-CAT, suggesting the importance of the PKCδ-independent protective activity of HSP25, which has been reported previously (44).

Interaction between HSP25 and PKCδ Correlates with Radioresistance in Lung Carcinoma Cell Lines—To determine the physiological relevance of the HSP25 and PKCδ interaction, three types of lung cancer cells with different HSP27 expressions and radioresistances were examined; NCI-H1299 showed highest HSP27 expression, and NCI-H460 least. HSP27 expression levels were found to correlate with radiation survival (Fig. 7*A*). When the interaction between HSP27 and PKCδ was checked by coimmunoprecipitating PKCδ and HSP27, a greater interaction between PKCδ and HSP27 and lower PKCδ kinase activity were found for NCI-H1299 than for NCI-H460 (Fig. 7*B*). When NCI-H1299 cells were treated with siRNA to HSP27, the HSP27-PKCδ interaction disappeared, and PKCδ kinase activity was restored (Fig. 7*C*). Cell death also increased after treating NCI-H1299 with HSP27 siRNA (Fig. 7*D*), sug-

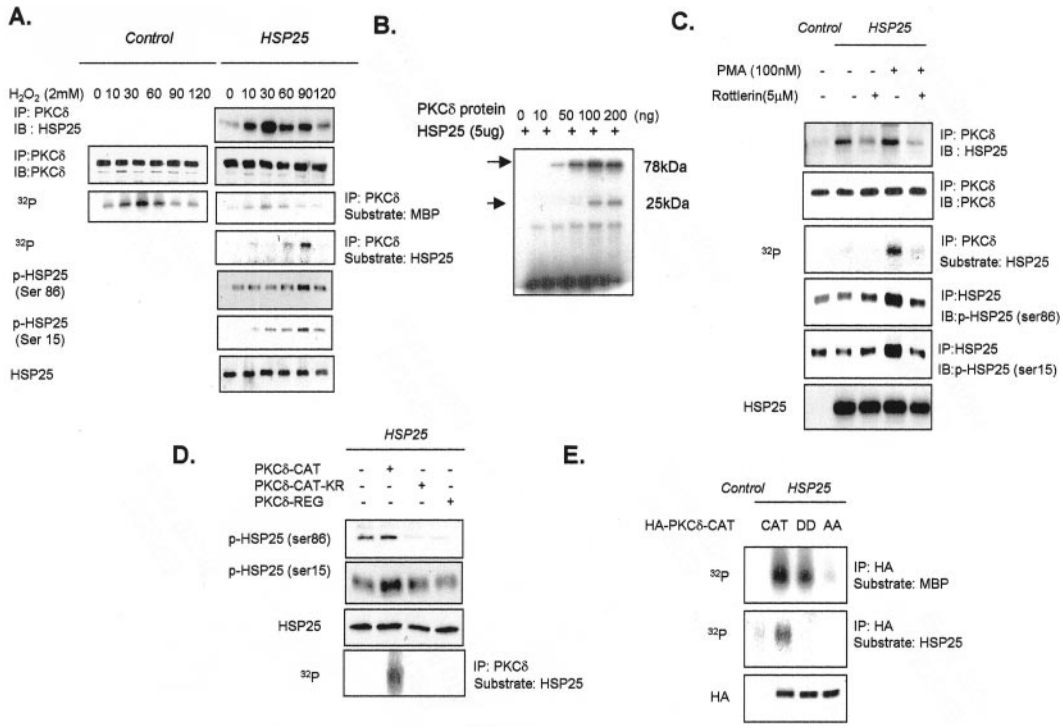

FIG. 5. **Interaction of PKCδ with HSP25 induces HSP25 phosphorylation.** *A*, immunoprecipitation (*IP*) of PKCδ in lysates from control or HSP25-overexpressing L929 cells after H_2O_2 (2 mM) pretreatment at the indicated time points. HSP25 or PKCδ protein was detected using anti-HSP25 or anti-PKCδ antibodies. Cellular proteins were extracted after lysis with PKC extraction buffer. PKC proteins from 300 μg of cell extracts were immunoprecipitated using anti-PKCδ antibody and protein G-Sepharose. Immune complex kinase reactions were performed in the presence of GST-MBP or His-HSP25 substrate and [γ-^{32}P]ATP. Western blotting was performed using anti-HSP25, anti-phospho-HSP25 (Ser-15), and anti-phospho-HSP25 (Ser-86) antibodies. *B*, the indicated amounts of recombinant PKCδ protein were immunoprecipitated using an anti-PKCδ antibody and protein G-Sepharose. Immune complex kinase reactions were performed in the presence of His-HSP25 substrate and [γ-^{32}P] with or without PKC lipid activator. *C*, immunoprecipitation of PKCδ in lysates from control or HSP25-overexpressing L929 cells treated with PMA (100 nM) and with or without rottlerin (5 μM). HSP25 or PKCδ proteins were detected using anti-HSP25 or PKCδ antibody. Cellular proteins were extracted after lysis using PKC extraction buffer. PKC proteins from 300 μg of cell extracts were immunoprecipitated using an anti-PKCδ antibody and protein G-Sepharose. Immune complex kinase reactions were performed in the presence of His-HSP25 substrate and [γ-^{32}P]ATP. Western blotting was performed using anti-HSP25, anti-phospho-HSP25 (Ser-15), and anti-phospho-HSP25 (Ser-86) antibodies after immunoprecipitating HSP25 with anti-HSP25 antibody. The light chain band of immunoglobulin G overlapped with the phospho-HSP25 band. *D*, Western blotting of lysates from PKCδ-CAT, PKCδ-CAT-KR, or PKCδ-REG in HSP25-overexpressing L929 cells was performed using anti-HP25, anti-phospho-HSP25 (Ser-15), or anti-phospho-HSP25 (Ser-86) antibodies after immunoprecipitating HSP25 with anti-HSP25 antibody. The light chain band of immunoglobulin G overlapped the phospho-HSP25 band. Cellular proteins were lysed and extracted using PKC extraction buffer. PKC proteins from 300 μg of cell extracts were immunoprecipitated using an anti-PKCδ antibody and protein G-Sepharose. Immune complex kinase reactions were performed in the presence of His-HSP25 substrate and [γ-^{32}P]ATP. *E*, cellular proteins were lysed and extracted using PKC extraction buffer from control or HSP25-overexpressing L929 cells after cotransfecting cells with HA-tagged PKCδ-CAT (*CAT*) or point mutants of PKCδ-CAT on S643D/S662D (*DD*) or S643A/S662A (*AA*). PKC proteins from 300 μg of cell extracts were immunoprecipitated using an anti-HA antibody and protein G-Sepharose. Immune complex kinase reactions were performed in the presence of GST-MBP or His-HSP25 substrate and [γ-^{32}P]ATP. The transfection efficiency of HA-tagged vectors was confirmed by Western blotting using anti-HA antibody. *IB*, immunoblot.

gesting that cell death inhibition is correlated with the level of interaction between HSP27 and PKCδ.

DISCUSSION

The coordinated interactions of kinases, phosphatases, and other regulatory molecules with scaffolding proteins is emerging as a major theme in intracellular signaling networks (45–47). Increasing numbers of types of PKC-binding proteins are now believed to play a role in directing the location and function of individual PKC isoforms to particular subcellular locations. In this study, we identified HSP25 as such a PKCδ-binding protein.

Small heat shock proteins are pleiotropic inhibitors of cell death whose physiological protective effects are observed mainly in stressed cells (11, 48–50). Several mechanisms have been proposed to account for this anti-apoptotic activity. HSP25 could raise defenses against oxidative stress by increasing glutathione content (51) or Mn-SOD enzyme activity (13). HSP27 also binds to activated Akt, a protein that generates a survival signal in response to growth factor stimulation (10, 52). Akt also inhibits cell death by phosphorylating and inactivating procaspase-9 (48) or by preventing the release of cytochrome *c* from mitochondria (6). HSP25 was also found to inhibit cell growth via the inhibition of PKCδ-mediated ERK1/2 activation (12, 14). Moreover, the present study identifies other mechanisms by which HSP25 interferes with cell death pathways. This cytoprotective activity is potentiated in the following two ways: by interaction between HSP25 and the V5 region of the catalytic domain of PKCδ, thereby preventing PKCδ-mediated cell death; and by interaction between kinase-active PKCδ and HSP25, which induces HSP25 phosphorylation at Ser-15 and Ser-86 and potentiates HSP25 cytoprotection.

In a previous study, we found that HSP25 inhibits PKCδ translocation to the membrane, the kinase activity, and tyrosine phosphorylation of PKCδ (14). In the present study, immunoprecipitation experiments were performed using HSP25-overexpressing L929 and Jurkat T cells, which do not express endogenous HSP25 or HSP27 protein. Most interestingly, HSP25 directly bound PKCδ in HSP25-overexpressing cells. HSP25/27 shares several properties with HSP70, another inducible HSP. When overexpressed, both stress proteins inhibit apoptosis *in vitro* and *in vivo*, induce resistance to most chemotherapeutic agents, and enhance tumorigenesis in rodents

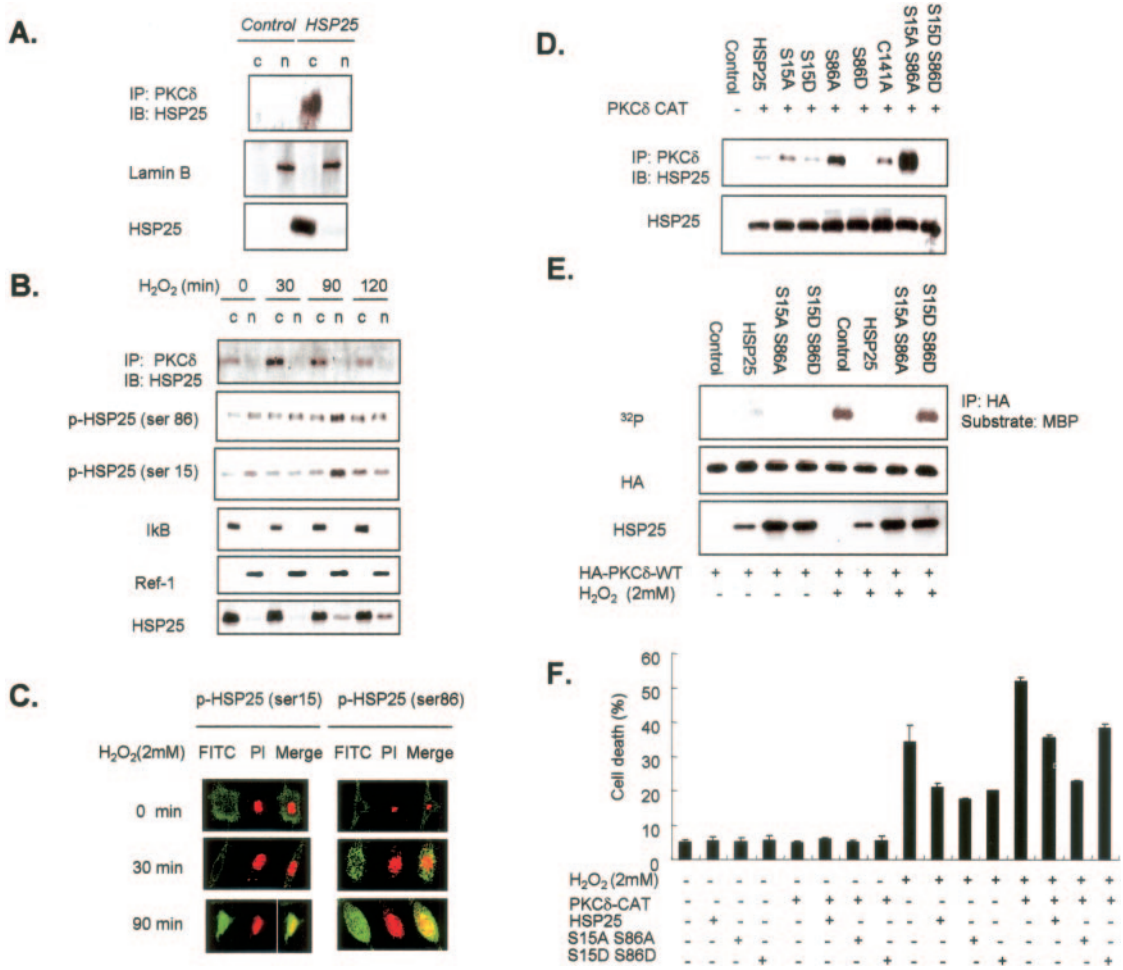

FIG. 6. **Unphosphorylated HSP25 preferentially binds to PKCδ and phosphorylated HSP25 produced by the HSP25-PKCδ interaction is translocated to the nucleus.** *A*, cytosolic (*c*) and nuclear (*n*) fractions of control and HSP25-overexpressing L929 cells were isolated; PKCδ was immunoprecipitated (*IP*) in lysates, and HSP25 protein was immunodetected using anti-HSP25 antibody. Nucleus specific protein lamin B was detected by Western blotting. *B*, cytosolic and nuclear fractions of HSP25-overexpressing L929 cells were isolated; PKCδ was immunoprecipitated from lysates, and HSP25 protein was immunodetected using anti-HSP25 antibody. Nucleus specific protein Ref-1, and cytosol-specific proteins IκB-α, phospho-HSP25 (Ser-15), and phospho-HSP25 (Ser-86) were detected by Western blotting. *C*, localization changes of phospho-HSP25 (Ser-15) and phospho-HSP25 (Ser-86) in L929 cells which stably overexpress HSP25 after treatment of H_2O_2 (2 mM). Cells were fixed with formaldehyde and immunostained with either anti-phospho-HSP25 (Ser-15) or anti-phospho-HSP25 (Ser-86) antibodies. The results shown are representative of two independent experiments. *D*, PKCδ was immunoprecipitated from the lysates of transfected L929 cells of control or vector containing either wild type HSP25 cDNA or the indicated point mutants with or without PKCδ-CAT cotransfection, and HSP25 protein was immunodetected using anti-HSP25 antibodies. *E*, cellular proteins were obtained using PKC extraction buffer from control or vector containing wild type HSP25 cDNA or the indicated point mutants cotransfected with HA-tagged PKCδ-WT in the presence or absence of H_2O_2 (2 mM). PKC proteins from 300 μg of cell extracts were immunoprecipitated using an anti-PKCδ antibody and protein G-Sepharose. Immune complex kinase reactions were performed in the presence of GST-MBP or His-HSP25 substrate and [γ-^{32}P]ATP. *F*, the cell deaths of L929 cells cotransfected with vector containing either wild type HSP25 cDNA or the indicated point mutants and PKCδ-CAT in the presence or absence of H_2O_2 (2 mM) were measured by flow cytometry after PI staining. Results are the means and standard deviations of three independent experiments. *IB*, immunoblot.

(49). However, several differences between these two chaperones have been identified. The first concerns ATP hydrolysis dependence. The second is that HSP70 as an early response gene and HSP25/27 is a late response gene. The third is that different molecular mechanisms are required for their anti-apoptotic effects (48). The present study also suggests that they differ in terms of their interaction with the PKCδ protein, although it should be noted that HSP70 did not bind PKCδ (data not shown). The PKCδ-binding site for HSP25 was PKCδ-CAT, and PKCδ kinase activity was important for the PKCδ-HSP25 interaction, because treatment with the PKCδ kinase inhibitor rottlerin, PKCδ-CAT-KR, or ATPγS inhibited the interaction between PKCδ and HSP25. An *in vitro* translation assay also confirmed the interaction between PKCδ-CAT and HSP25.

Because PKCδ has been reported to induce cell death with the concomitant activation of PKCδ or PKCδ tyrosine phosphorylation (36, 53, 54) and HSP25 was found to inhibit cell death (Fig. 2), we concluded that the interaction between kinase-active PKCδ-CAT and HSP25 inhibits PKCδ activity and PKCδ-mediated cell death. When the binding sites of HSP25 and PKCδ-CAT were investigated using deletion mutants of PKCδ or HSP25, we found that amino acids 90–103 of HSP25 and the V5 region (amino acids 630–674 of PKCδ) of PKCδ (Figs. 4 and 5) are essential for the interaction between HSP25 and PKCδ. Amino acids 92–145 of HSP25 are overlapping with the cytochrome *c*-binding site (7) and with the 26 S proteosomal PA700-binding site (8), which suggests that the β-sheets of the α-crystalline domain of HSP25/27 (indispensable for the HSP25/27 chaperone function *in vitro* (55)) might also be important for the interaction between HSP25 and PKCδ. Moreover, the deletion of amino acids 90–103 in the HSP25 sequence inhibited HSP25-mediated cytoprotection, suggesting that binding between HSP25 and PKCδ is required for the HSP25-mediated cytoprotection (Fig. 3). Because the 90–103-amino acid region of HSP25 overlaps the cytochrome *c*-binding

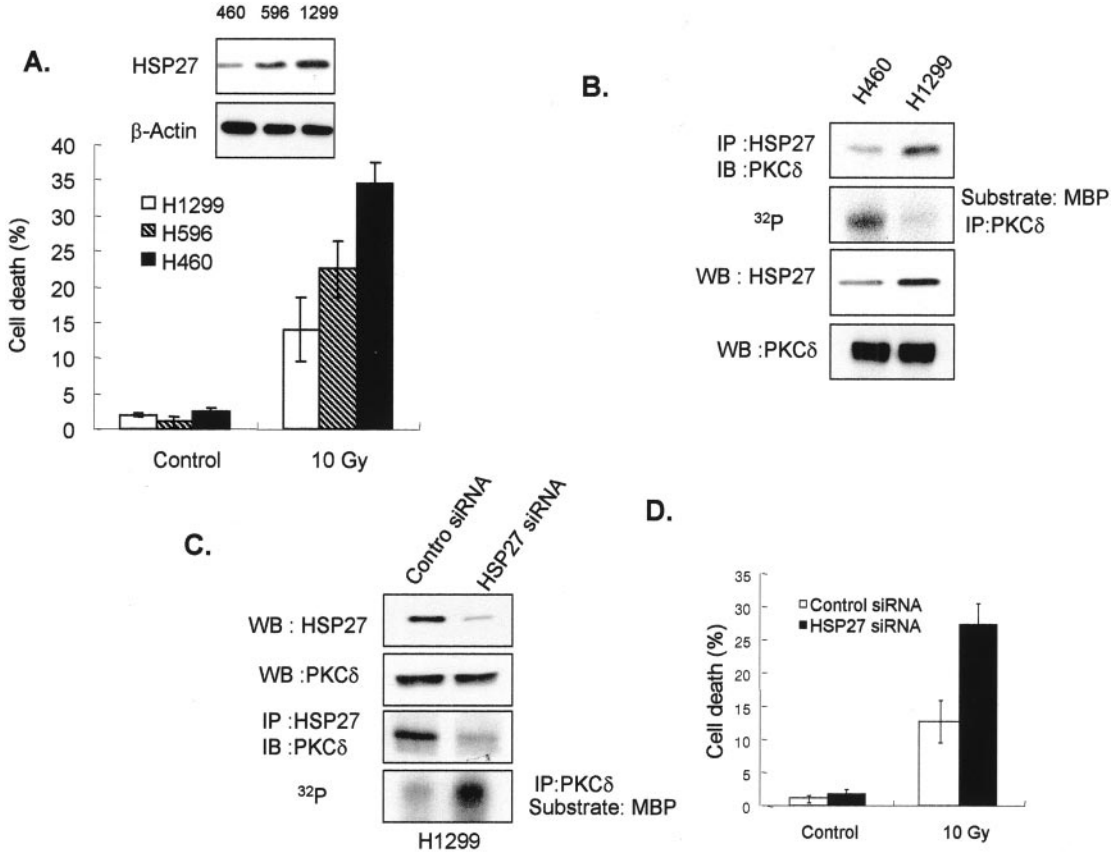

FIG. 7. **The interaction between HSP25 and PKCδ correlates with radioresistance.** *A*, the cell deaths of the human lung carcinoma cell lines, NCI-H460, -H596, and -H1299 after 10 Gy of γ-radiation exposure was measured by flow cytometric analysis after PI staining. Results are the means ± S.D. of three independent experiments. Western blotting (*WB*) was performed using anti-HSP27 antibody. *B*, HSP27 was immunoprecipitated (*IP*) in lysates from NCI-H460, and-H1299 with anti-PKCδ antibodies. Cellular proteins were extracted by lysis using PKC extraction buffer, and PKC proteins were immunoprecipitated from 300 μg of cell extracts using anti-PKCδ antibody and protein G-Sepharose. Immune complex kinase reactions were performed in the presence of GST-MBP substrate and [γ-^{32}P]ATP. *C*, immunoprecipitation of HSP27 from lysates of NCI-H1299 after transfection with control siRNA or HSP27 siRNA; PKCδ protein was immunodetected using anti-PKCδ antibodies. Cellular proteins were obtained by lysing and then extracting with PKC extraction buffer. PKC proteins from 300 μg of cell extracts were immunoprecipitated using anti-PKCδ antibody and protein G-Sepharose. Immune complex kinase reactions were performed in the presence of GST-MBP substrate and [γ-^{32}P]ATP. *D*, NCI-H1299 cell death after transfecting with control siRNA or HSP27 siRNA with or without exposure to 10 Gy of gamma radiation was measured by flow cytometry after PI staining. Results are the means ± S.D. of three independent experiments. *IB*, immunoblot.

site (amino acids 51–141 of HSP27) and the PA700-binding site (amino acids 88–141 of HSP27), this cytoprotective effect represents more than an inhibition of PKCδ-mediated activity. Moreover, it appears reasonable to conclude that the inhibition of PKCδ-mediated cell death by HSP25 interaction with PKCδ is involved in the inhibition of cell death by HSP25.

Oxidative stress or ionizing radiation permits PKC to translocate to the membrane in an open conformation, allowing its pseudosubstrate region to be released from its substrate-binding cavity and enabling C-terminal access to the substrate-binding site and autophosphorylation at Ser-643 and Ser-662 by intramolecular mechanisms, which activates downstream signaling (56). Because HSP70 has been reported to interact with the dephosphorylated turn motif of PKCβ II, we examined whether PKCδ interacts with HSP25 in a similar manner. Phosphorylation-deficient mutants but not phosphorylation-mimicking mutants of the V5 region of PKCδ were found to bind to HSP25. Moreover, HSP25 inhibited PKCδ translocation to the particulate fraction (Fig. 4), suggesting that the primed activation of PKCδ permits V5 regions to be exposed, autophosphorylated, and fully activated. As soon as the V5 region is exposed and before autophosphorylation at Ser-643 and Ser-662, HSP25 may bind to the V5 region of PKCδ to stabilize PKCδ and thus inhibit re-phosphorylation and re-activation. Thus, PKCδ activity and its translocation to the particulate fraction are inhibited by the PKCδ-HSP25 interaction.

HSP25 is regulated by post-translational modifications like phosphorylation, deamination, and acylation (42). Moreover, the phosphorylation of HSP25 is catalyzed by MAPK-activated protein kinase 2/3 (a serine protein kinase), which is phosphorylated and activated by p38 MAPK or EKR1/2 (44, 57), in a stress-dependent manner. In addition, the inhibition of HSP25 phosphorylation resulted in the destruction of actin filaments and the blocking of the protective effect mediated by HSP25 under heat shock conditions, suggesting that the phosphorylation of HSP25 is important for the stability of actin filament and for thermoresistance (44). In the present study, we found for the first time, that PKCδ induces HSP25 phosphorylation at Ser-15 and Ser-86 and that the direct interaction between PKCδ and HSP25 induces HSP25 phosphorylation (Fig. 5). However, it remains to be determined why PKCδ phosphorylated MBP before HSP25. One possibility is that the phosphorylation of HSP25 by PKCδ, unlike the phosphorylation of MBP by PKCδ, requires structural changes in the PKCδ-HSP25 complex. Indeed, PKCδ activation may expose the V5 region of PKCδ, and HSP25 then binds directly to this region to induce some conformational change. Another possibility is that PKCδ has a different substrate binding affinity, and thus the kinetics of the phosphorylations of MBP or HSP25 by PKCδ may differ.

The interaction between PKCδ and HSP25 usually occurred

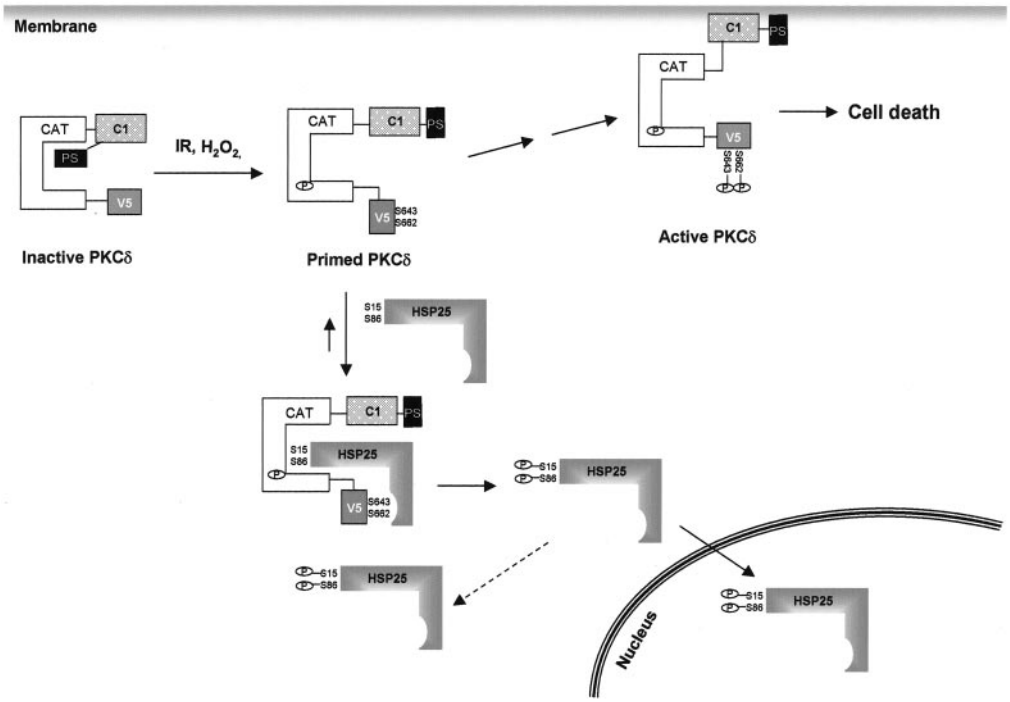

FIG. 8. **Hypothetical scheme for the role of HSP25 in the inhibition of PKCδ-mediated apoptosis.** In response to a stimulus, such as radiation (*IR*) or oxidative stress, PKCδ is primed for activation by PDK-1 and tyrosine kinase, and then the V5 region is exposed. Primed PKCδ becomes fully active by the autophosphorylation of Ser-643 and Ser-662 in the V5 region and by membrane translocation. HSP25 directly binds to the exposed V5 region of PKCδ, which inhibits PKCδ activity by blocking the autophosphorylation of PKCδ at Ser-662 and Ser-643 and its subsequent translocation to the membrane fraction, which is correlated with the induction of apoptosis. The interaction between PKCδ and HSP25 also induces HSP25 phosphorylation at Ser-15 and Ser-86, and this phosphorylation facilitates the dissociation of phosphorylated HSP25 from PKCδ. Phosphorylated HSP25 translocates to the nucleus, although some remains in the cytoplasm. When HSP25 is overexpressed, apoptotic induction by radiation or oxidative stress is inhibited because PKCδ remains bound to HSP25.

in cytosol (Fig. 6), and phosphorylated HSP25 was translocated to the nucleus. The results of our kinetic experiments involving H_2O_2 additions and phosphorylation-deficient mutants of HSP25 at Ser-15 and Ser-86 suggest that exposed V5 regions of PKCδ after activation interact with unphosphorylated HSP25 in the cytosol and that after phosphorylation by PKCδ, phosphorylated HSP25 translocates to the nucleus.

The physiological importance of the correlation between PKCδ-HSP25 binding and radioresistance in lung carcinoma cell lines implies that HSP27 overexpression, which is related to radioresistance (Fig. 7), is in part determined by the HSP25/27-PKCδ interaction. Because HSP27 expression in lung carcinoma cells is well correlated with radioresistance, the V5 region of PKCδ might be therapeutically useful for inhibiting radioresistance by HSP27.

PKCδ activity plays an essential role in the apoptosis of cells, and small HSP is constitutively expressed in many cancer cells to negatively regulate apoptotic induction. The small HSP-PKCδ interaction could thus indicate the physiologic importance of this small HSP (Fig. 8). Moreover, this property might account for the observed protective effect of this protein when induced in response to radiation or oxidative stress.

REFERENCES

1. Wagstaff, M. J., CollacoMoraes, Y., Smith, J., de Belleroche, J. S., Coffin, R. S., and Latchman, D. S. (1999) *J. Biol. Chem.* **274,** 5061–5069
2. Guay, J., Lambert, H., Gingras-Breton, G., Lavoie, J. N., Huot, J., and Landry, J. (1997) *J. Cell Sci.* **110,** 357–368
3. Huot, J., Houle, F., Marceau, F., and Landry, J. (1997) *Circ. Res.* **80,** 383–392
4. Landry, J., and Hout, J. (1999) *Biochem. Soc. Symp.* **64,** 79–80
5. Mehlen, P., Coronas, V., Ljubic-Thibal, V., Ducasse, C., Granger, L., Jourdan, F., and Arrigo, A. P. (1999) *Cell Death Differ.* **6,** 227–233
6. Paul, C., Manero, F., Gonin, S., Kretz-Remy, C., Virot, S., and Arrigo, A. P. (2002) *Mol. Cell. Biol.* **22,** 816–834
7. Bruey, J. M., Ducasse, C., Bonniaud, P., Ravagnan, L., Susin, S. A., Diaz-Latoud, C., Gurbuxani, S., Arrigo, A. P., Kroemer, G., Solary, E., and Garrido, C. (2000) *Nat. Cell Biol.* **2,** 645–652
8. Parcellier, A., Schmitt, E., Gurbuxani, S., Seigneurin-Berny, D., Pance, A., Chantome, A., Plenchette, S., Khochbin, S., Solary, E., and Garrido, C. (2003) *Mol. Cell. Biol.* **23,** 5790–5802
9. Charette, S. J., and Landry, J. (2000) *Ann. N. Y. Acad. Sci.* **926,** 126–131
10. Rane, M. J., Pan, Y., Singh, S., Powell, D. W., Wu, R., Cummins, T., Chen, Q., Leish, K. R., and Klein, J. B. (2003) *J. Biol. Chem.* **278,** 27828–27835
11. Park, S. H., Cho, H. N., Lee, S. J., Kim, T. H., Lee, Y., Park, Y. M., Lee, Y. J., Cho, C. K., Yoo, S. Y., and Lee, Y. S. (2000) *Radiat. Res.* **154,** 421–428
12. Cho, H. N., Lee, S. J., Park, S. H., Lee, Y. J., Cho, C. K., and Lee, Y. S. (2001) *Int. J. Radiat. Biol.* **77,** 225–233
13. Yi, M. J., Park, S. H., Cho, H. N., Chung, H. Y., Kim, J. I., Cho, C. K., Lee, S. J., and Lee, Y. S. (2002) *Radiat. Res.* **158,** 641–649
14. Lee, Y. J., Cho, H. N., Jeoung, D. I., Soh, J. W., Cho, C. K., Bae, S., Chung, H. Y., Lee, S. J., and Lee, Y. S. (2004) *Free Radic. Biol. Med.* **36,** 429–444
15. Lee, Y. J., Lee, D. H., Cho, C. K., Chung, H. Y., Bae, S., Jhun, G. J., Soh, J. W., Jeoung, D. I., Lee, S. J., and Lee, Y. S. (2005) *Oncogene,* in press
16. Cho, H. N., Lee, Y. J., Cho, C. K., Lee, S. J., and Lee, Y. S. (2002) *Cell Death Differ.* **9,** 448–456
17. Watanabe, T., Ono, Y., Taniyam, Y., Hazama, K., Igarashi, K., Ogita, K., Kikkawa, U., and Nishizuka, Y. (1992) *Proc. Natl. Acad. Sci. U. S. A.* **89,** 10159–10163
18. Lu, Z., Hornia, A., Jiang, Y. W., Zang, Q., Ohno, S., and Foster, D. A. (1997) *Mol. Cell. Biol.* **17,** 3418–3428
19. Cross, T., Griffiths, G., Deacon, E., Sallis, R., Gough, M., Watters, D., and Lord, M. (2000) *Oncogene* **19,** 2331–2337
20. Basu, A., Woolard, M. D., and Johnson, C. L. (2001) *Cell Death Differ.* **8,** 899–908
21. Denning, M. F., Wang, Y., Tibudan, S., Alkan, S., Nickoloff, B. J., and Qin, J. Z. (2002) *Cell Death Differ.* **9,** 40–52
22. Yuan, Z., Ishiko, T., Nakada, S., Huang, Y., Kharbanda, S., Weischselbaum, R., and Kufe, D. (1998) *Oncogene* **16,** 1643–1648
23. Reyland, M. E., Anderson, S. M., Matassa, A. A., Barzen, K. A., and Quissell, D. O. (1999) *J. Biol. Chem.* **274,** 19115–19123
24. Godbout, J. P., Pesavento, J., Hartman, M. E., Manson, S. R., and Freund, G. C. (2002) *J. Biol. Chem.* **277,** 2554–2561
25. Ghayur, T., Hugunin, M., Talanian, R. V., Ratnofsky, S., Quinlan, C., Emoto, Y., Pandey, P., Datta, R., Huang, Y., Kharbanda, S., Allen, H., Kamen, R., Wong, W., and Kufe, D. (1996) *J. Exp. Med.* **184,** 2399–2404
26. Mizuno, K., Noda, K., Araki, T., Imaoka, T., Kobayashi, Y., Akita, Y., Shimonaka, M., Kishi, S., and Ohno, S. (1997) *Eur. J. Biochem.* **250,** 7–18
27. Matassa, A. A., Carpenter, L., Biden, T. J., Humphries, M. J., and Reyland, M. E. (2001) *J. Biol. Chem.* **276,** 29719–29728
28. Leverrier, S., Vallentin, A., and Joubert, D. (2002) *Biochem. J.* **368,** 905–913
29. Ho, S. N., Hunt, H. D., Horton, R. M., Pullen, J. K., and Pease, L. R. (1989) *Gene* (*Amst.*) **77,** 51–59
30. Soh, J. W., Lee, E. H., Prywes, R., and Weinstein, I. B. (1999) *Mol. Cell. Biol.* **19,** 1313–1324
31. Ory, D. S., Neugeboren, B. A., and Mulligan, R. C. (1996) *Proc. Natl. Acad. Sci.*

U. S. A. **93,** 11400–11406
32. Gao, T., and Newton, A. C. (2002) *J. Biol. Chem.* **277,** 31585–31592
33. Shimabukuro, K., Yasuda, R., Muneyuki, E., Hara, K. Y., Kinosita, K., Jr., and Yoshida, M. (2003) *Proc. Natl. Acad. Sci. U. S. A.* **100,** 14731–14736
34. Lee, Y. J., Soh, J. W., Dean, N. M., Cho, C. K., Kim, T. H., Lee, S. J., and Lee, Y. S. (2002) *Cell Growth & Differ.* **13,** 237–246
35. Li, W., Zhang, J., Bottaro, D. P., and Pierce, J. H. (1997) *J. Biol. Chem.* **272,** 24550–24555
36. Blass, M., Kronfeld, I., Kazimirsky, G., Blumberg, P. M., and Brodie, C. (2002) *Mol. Cell. Biol.* **22,** 182–195
37. Li, W., Mischak, H., Yu, J. C., Wang, L. M., Mushinski, J. F., Heidaran, M. A., and Pierce, J. H. (1994) *J. Biol. Chem.* **269,** 2349–2352
38. Stempka, L., Schnolzer, M., Radke, S., Rincke, G., Marks, F., and Gschwendt, M. (1999) *J. Biol. Chem.* **274,** 8886–8892
39. Parekh, D., Ziegler, W., Yonezawa, K., Hara, K., and Parker, P. J. (1999) *J. Biol. Chem.* **274,** 34758–34764
40. Dutil, E. M., Keranen, L. M., DePaoli-Roach, A. A., and Newton, A. C. (1994) *J. Biol. Chem.* **269,** 29359–29362
41. Wang, Q. J., Lu, G., Schlapkohl, W. A., Goerke, A., Larsson, C., Mischak, H., Blumberg, P. M., and Mushinski, J. F. (2004) *Mol. Cancer Res.* **2,** 129–140
42. Welsh, M. J., and Gaestel, M. (1998) *Ann. N. Y. Acad. Sci.* **851,** 28–35
43. Knauf, U., Jakob, U., Engel, K., Buchner, J., and Gaestel, M. (1994) *EMBO J.* **13,** 54–60
44. Geum, D., Son, G. H., and Kim, K. (2002) *J. Biol. Chem.* **277,** 19913–19921
45. Dutil, E. M., Toker, A., and Newton, A. C. (1998) *Curr. Biol.* **6,** 806–809
46. Pawson, T., and Scott, J. D. (1997) *Science* **278,** 2075–2080
47. Jaken, S., and Parker, P. J. (2000) *BioEssays* **22,** 245–254
48. Garrido, C., Bruey, J. M., Fromentin, A., Hammann, A., Arrigo, A. P., and Solary, E. (1999) *FASEB J.* **13,** 2061–2070
49. Garrido, C., Fromentin, A., Bonnotte, B., Favre, N., Moutet, M., Arrigo, A. P., Mehlen, P., and Solary, E. (1998) *Cancer Res.* **58,** 5495–5499
50. Garrido, C., Ottavi, P., Fromentin, A., Hammann, A., Arrigo, A. P., Chauffert, B., and Mehlen, P. (1997) *Cancer Res.* **57,** 2661–2667
51. Baek, S. H., Min, J. N., Park, E. M., Han, M. Y., Lee, Y. S., Lee, Y. J., and Park, Y. M. (2002) *J. Cell. Physiol.* **183,** 100–107
52. Konishi, H., Matsuzaki, H., Tanaka, M., Takemura, Y., Kuroda, S., Ono, Y., and Kikkawa, U. (1997) *FEBS Lett.* **410,** 493–498
53. Fujii, T., Garcia-Bermejo, M. L., Bernabo, J. L., Caamano, J., Ohba, M., Kuroki, T., Li, L., Yuspa, S. H., and Kazanietz, M. G. (2000) *J. Biol. Chem.* **275,** 7574–7582
54. Pongracz, J., Webb, P., Wang, K., Deacon, E., Lunn, O. J., and Lord, J. M. (1999) *J. Biol. Chem.* **274,** 37329–37334
55. Guo, Z., and Cooper, L. F. (2000) *Biochem. Biophys. Res. Commun.* **270,** 183–189
56. Newton, A. C. (2003) *Biochem. J.* **370,** 361–371
57. Maizels, E. T., Peters, C. A., Kline, M., Cutler, R. E., Shanmugam, M., and Hunzicker-Dunn, M. (1998) *Biochem. J.* **332,** 703–712

HSP25 Inhibits Protein Kinase Cδ-mediated Cell Death through Direct Interaction

Yoon-Jin Lee, Dae-Hoon Lee, Chul-Koo Cho, Sangwoo Bae, Gil-Ja Jhon, Su-Jae Lee, Jae-Won Soh and Yun-Sil Lee

J. Biol. Chem. 2005, 280:18108-18119.
doi: 10.1074/jbc.M501131200 originally published online February 24, 2005
